

# Consequences of the Formation of an Organometallic Exciplex $[\text{Hg}(\eta^2\text{-arene})]$ in Mercury-Photosensitized Reactions of Arenes: C–C, C–O, and C–N Bond Cleavage

Lissa A. Fowley, Jesse C. Lee, Jr., and Robert H. Crabtree\*

Department of Chemistry, Yale University, New Haven, Connecticut 06520-8107

Per E. M. Siegbahn\*

Department of Physics, University of Stockholm, Box 6730, S-113 85 Stockholm, Sweden

Received September 5, 1995<sup>Ⓢ</sup>

We have previously shown that mercury-photosensitized reactions give an unexpected C–C bond cleavage for  $\text{PhCH}_2\text{-CH}_3$  and related aromatic systems. In this paper we report further theoretical and experimental studies that demonstrate the importance of organometallic intermediates of the type  $^3[\text{Hg}(\eta^2\text{-ArR})]$  in this chemistry and suggest how the C–C cleavage reaction occurs. We also find that in addition to these C–C bond cleavage reactions, analogous C–O and C–N bond cleavages can also occur with the following preference order for bond cleavage: C–O > C–N > C–C.

## Introduction

We have previously described conditions which allow us to dehydrodimerize organic compounds on a preparative scale by Hg-photosensitized reaction in the vapor phase via a C–H bond cleavage pathway.<sup>1,2</sup> Conditions have been identified that make these Hg-photosensitized reactions synthetically efficient for a variety of different types of substrate. For alkane substrates, we have shown in theoretical work that C–H activation by the  $^3\text{P}_1$  excited state ( $\text{Hg}^*$ ) proceeds by initial formation of weak  $[\text{Hg}^*(\text{alkane})]$  exciplexes, bound by 2–6 kcal/mol, followed by a direct interaction between the 6s and 6p orbitals of  $\text{Hg}^*$ .<sup>3</sup> The C–H cleavage mechanism can be described as a mixture of oxidative addition and abstraction but is dominated by oxidative addition. For example, the C–H activation transition state found for propane is easily accessible, being only 4.9 kcal/mol higher than the reactant energy. In principle, C–C activation could proceed the same way, but in practice, alkane C–C cleavage with  $\text{Hg}^*$  has high barriers theoretically and no reaction was observed experimentally. The explanation seems to be that  $\text{RCH}_2\text{-}$  groups in  $\text{RCH}_2\text{-CH}_2\text{R}$  (R = alkyl) have directed bonds, and in an oxidative addition mechanism *two* of these groups need to be tilted before an effective interaction with the  $\text{Hg}^*$  orbitals can take place. In contrast, for the activation of  $\text{RCH}_2\text{-H}$  bonds, only one alkyl group needs to

be tilted, H having a spherical 1s orbital. For the hydrogen molecule, the spherical nature of the hydrogen atom leads to a very low activation barrier for the H–H bond. With an oxidative addition mechanism,  $\text{Hg}^*$  attack can occur at hydrogen both for  $\text{H}_2$  and for C–H activation of alkanes but has to occur at an alkyl group for C–C activation of alkanes. In this case, the alkyl group is required to invert somewhat in order to effectively interact with  $\text{Hg}^*$ . With both mechanisms C–H activation should therefore be preferred over C–C activation of alkanes as is indeed found experimentally.

In a previous paper, we showed that alkylarenes of type  $\text{ArCH}_2\text{-CH}_2\text{R}$  (Ar = aryl; R = H, alkyl) are exceptional in reacting with  $\text{Hg}^*$  to give C–C activation of the  $\alpha,\beta\text{-C-C}$  bond in competition with  $\alpha\text{-C-H}$  activation.<sup>4</sup> We previously proposed that exciplex formation leads to triplet sensitization of the arene, followed by C–C bond cleavage. Theoretical work indicated a  $^3[\text{Hg}^*(\eta^2\text{-C}_6\text{H}_6)]$  structure for the exciplex, which is bound by a substantial 29.9 kcal/mol with respect to  $\text{Hg}^*$  and benzene (Figure 1).

In this paper we continue the investigation of  $\text{Hg}^*$ -mediated C–C bond cleavage by studying a number of arenes in detail. We also extend our experimental studies to the case of  $\text{ArCH}_2\text{-X}$  (X = OH and  $\text{NH}_2$ ) and related compounds where we find that C–O and C–N cleavage occurs even more readily than in the X =  $\text{CH}_3$  case.

## Results and Discussion

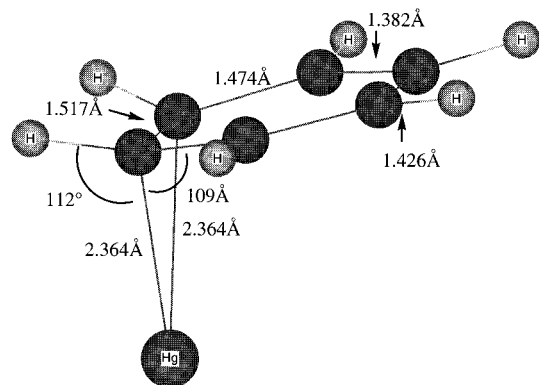
**Experimental Results in C–C Cleavage. Simple Arenes.** In our initial experiments we demonstrated that benzene, toluene, and *p*-xylene all react via C–H bond cleavage to give the corresponding dehydrodimers, biphenyl (24%), bibenzyl (67%), and 1,2-di-*p*-tolylethane

<sup>Ⓢ</sup> Abstract published in *Advance ACS Abstracts*, January 1, 1996. (1) (a) Brown, S. H.; Crabtree, R. H. *Tetrahedron Lett.* **1987**, *28*, 5599. (b) Brown, S. H.; Crabtree, R. H. *J. Chem. Educ.* **1988**, *65*, 290. (c) Brown, S. H.; Crabtree, R. H. U.S. Patent 3,725,342. (d) Brown, S. H.; Crabtree, R. H. *J. Am. Chem. Soc.* **1989**, *111*, 2935. (e) Muedas, C. A.; Ferguson, R. R.; Crabtree, R. H. *Tetrahedron Lett.* **1989**, *30*, 3389. (f) Boojamra, C. G.; Crabtree, R. H.; Ferguson, R. R.; Muedas, C. A. *Tetrahedron Lett.* **1989**, *30*, 5583.

(2) (a) Ferguson, R. R.; Boojamra, C. G.; Brown, S. H.; Crabtree, R. H. *Heterocycles* **1989**, *28*, 121. (b) Ferguson, R. R.; Crabtree, R. H. *New J. Chem.* **1989**, *13*, 647. (c) Muedas, C. A.; Ferguson, R. R.; Brown, S. H.; Crabtree, R. H. *J. Am. Chem. Soc.* **1991**, *113*, 2233. (d) Ferguson, R. R.; Krajnik, P.; Crabtree, R. H. *Syn Lett.* **1991**, *9*, 597. (e) Lee, J. C., Jr.; Boojamra, C. G.; Crabtree, R. H. *J. Org. Chem.* **1993**, *58*, 3895.

(3) Siegbahn, P. E. M.; Svensson, M.; Crabtree, R. H. *J. Am. Chem. Soc.*, in press.

(4) Fowley, L. A.; Lee, J. C., Jr.; Crabtree, R. H.; Siegbahn, P. E. M. *J. Organomet. Chem.* **1995**, *504*, 57.



**Figure 1.** Structure of the  $[\text{Hg}(\eta^2\text{-C}_6\text{H}_6)]$  exciplex from quantum chemical calculations. Hg–C and C–C distances are shown.

**Table 1**

Substrate	Major Products	Rate of Dimer Formation (mg/h)
	24%	0.52
	67%	0.47
	58%	1.5
	73%	0.93

(58%), respectively (Table 1).<sup>5</sup> When a monosubstituted arene contained an alkyl chain longer than methyl, a substantial amount of C–C bond cleavage at the  $\text{ArCH}_2\text{-CH}_2\text{R}$  position was observed. To quantify C–C bond cleavage in the products, we have compared the ratio of  $R_{\text{CH}}$  groups, formed by C–H bond breaking, to  $R_{\text{CC}}$  groups, formed by C–C bond breaking. We have defined an  $r$  factor:

$$r_{\text{CC}} = (R_{\text{CC}})/(R_{\text{CH}})$$

where  $R_{\text{CC}}$  and  $R_{\text{CH}}$  represent the number of moles of each type of R group in the products.

Several general trends were seen for a variety of aromatic substrates (Table 2). C–C bond cleavage was seen for all monosubstituted PhR compounds. As chain length increased, a decrease was seen in the magnitude of  $r_{\text{CC}}$ . Likewise, as the stability of the departing aliphatic radical increased, the magnitude of  $r_{\text{CC}}$  rose rapidly, implying that stabler radicals are better leaving groups in the reaction. Oxygenated products were detected in some cases, usually associated with involatile aromatic substrates where trace  $\text{O}_2$  trapped some of the radical intermediates. No disubstituted arenes ever gave any C–C bond cleavage, including those with fused ring systems. Last, the aliphatic C radicals

(5) These percentages refer to the mole fraction of the arene products formed in the final product mixture of involatile materials after the photochemical step. This number is not a yield, because excess arene is always used, some of which is entrained by the gas stream and lost from the apparatus; some of the arene disproportionation products are also lost this way. These percentage values and weights of the involatile fraction formed per hour were repeatable while numbers for yields were not, because of differential losses of starting materials in different experiments.

released in the C–C bond cleavage reaction were found to add to the aromatic ring, especially in the case of substrates yielding the more stable aliphatic radicals such as *t*-Bu, which gave the highest amounts of ring addition products. In addition, we investigated the dehydrodimerization of mesitylene to see if substitution of the arene ring would affect the reactivity in a C–H bond cleavage reaction, but rates for mesitylene dimerization were comparable to those for other simple arenes (Table 1).

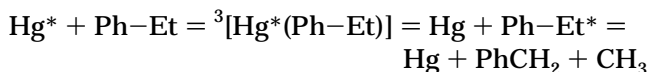
**Other Examples of C–C Bond Cleavage.** 4-Phenyl-1-butene gave 64% C–C bond cleavage products, giving an  $r_{\text{CC}}$  value of 3.30 (Table 3). This value is much higher than that of *n*-butylbenzene ( $r_{\text{CC}} = 0.042$ ), probably due to the stability of the allyl radical formed from C–C bond cleavage. This supports the idea that a stabler radical is more easily cleaved, increasing the value of  $r_{\text{CC}}$ .

In an attempt to form an intramolecular diradical upon C–C bond cleavage, cyclopropylbenzene and cyclohexylbenzene were examined under Hg photosensitized conditions. Cyclopropylbenzene led only to oxygenated products (both cyclic and ring opened alcohols) and various dimers. No products of rearrangement to indane were seen. In the case of cyclohexylbenzene, only the cyclic alcohol was detected in good yield (Table 3).

In the case of methyl phenylacetate, the radical formed on C–C cleavage is expected to be  $\cdot\text{CO}_2\text{CH}_3$ . The  $r_{\text{CC}}$  value for the reaction was found to be high (2.98), suggesting that the C– $\text{CO}_2\text{Me}$  bond is weak.

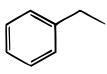
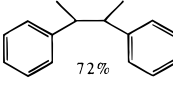
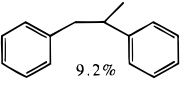
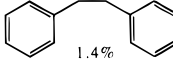
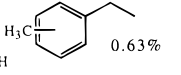
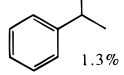
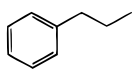
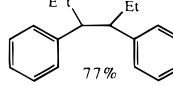
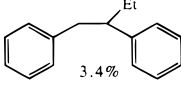
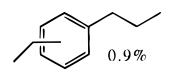
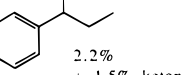
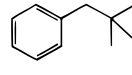
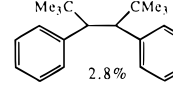
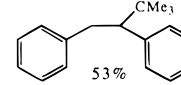
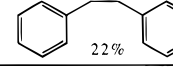
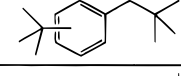
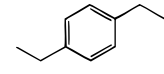
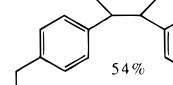
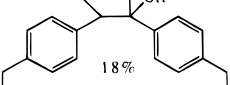
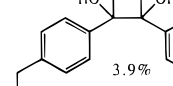
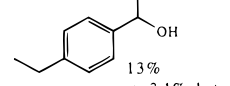
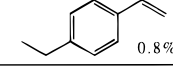
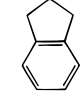
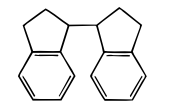

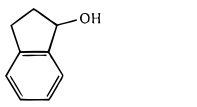
**Theoretical Investigation of C–C Cleavage. The Case of Ethane.** In the previous theoretical study, no transition state was located for ethane and  $\text{Hg}^*$  but it was concluded that the barrier for C–C activation is quite high.<sup>3</sup> A somewhat more detailed study of this reaction has now been made. Since it is very difficult to obtain convergence for a transition state, we chose a simple reaction coordinate, the C–C distance, which was elongated in increments of 0.2 Å, all other coordinates then being optimized. The PCI-80 energy for the highest point [ $d(\text{C}-\text{C}) = 2.0$  Å] led to an estimated barrier of 26.1 kcal/mol for C–C activation after applying zero-point and spin-orbit corrections. This barrier, although approximate, is clearly much too high for facile reaction, in line with the experimental absence of C–C bond cleavage for alkanes under our conditions. The transition-state Hg–C bond distances are somewhat unequal (2.44 and 2.58 Å), indicating a mixture of oxidative addition and abstraction but with a clear dominance of oxidative addition.

**The Case of Alkylarenes.** Calculations for Ph–Et suggest the reaction occurs in several steps: exciplex formation, triplet energy transfer, and then C–C cleavage in the triplet arene.



The results at both the PCI-80 level and the B3LYP level are given in Table 4. In the first step of the reaction, already discussed in ref 4, an organometallic exciplex of structure  $[\text{Hg}(\eta^2\text{-ArR})]^*$  is formed, as illustrated in Figure 1 for the case of benzene. The

Table 2

Substrate	Major Products	Rate of Product Formation (mg/h)	$\tau$
	 72%  9.2%  1.4%  0.63%  1.3%	0.5	0.15
	 77%  3.4%  0.9%  2.2% + 1.5% ketone	1.1	0.044
	 2.8%  53%  2.2%  2.5%	1.4	4.1
	 54%  18%  3.9%  13% + 3.1% ketone  0.8%	2.5	0.0
	 50%  2.1%  7.3% + 4.8% ketone	5.3	0.0

binding energy obtained for benzene was 29.9 kcal/mol and that for Ph-Et should be very similar. Since the calculated PCI-80 excitation energy between Hg and Hg\* is 109.5 kcal/mol (experimental, 112.7 kcal/mol), the  $^3[\text{Hg}^*(\text{Ph-Et})]$  complex is 79.6 kcal/mol above Hg and Ph-Et. This value is somewhat lower than the calculated excitation energy for Ph-Et to the lowest triplet excited state Ph-Et\* of 87.3 kcal/mol. The exciplex is thus only bound by 7.7 kcal/mol with respect to Hg and Ph-Et\*. The wave function, discussed in ref 4, is closer to those of Hg and Ph-Et\*, and so this exciplex is perhaps best considered  $^3[\text{Hg}(\text{Ph-Et}^*)]$ , with the organic group having triplet character. The energetics of the system are shown in Figure 2.

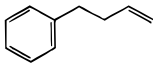
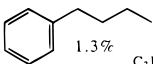
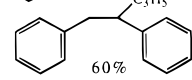
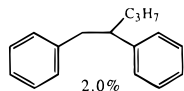
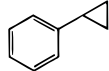
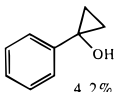
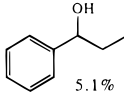
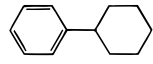
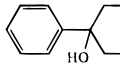
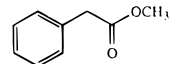
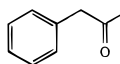
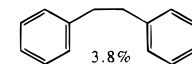
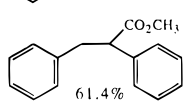
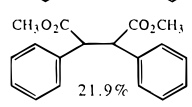
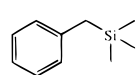
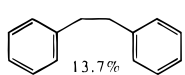
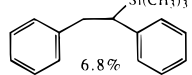
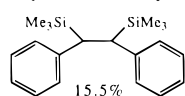
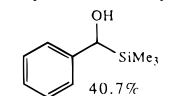
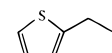
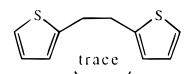
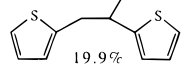
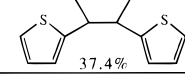
**Vibrational Excitation of the Triplet Arene.** A key point is that, on dissociation of the exciplex, the newly formed Ph-Et\* triplet has a large excess vibrational energy on the order of 30 kcal/mol. Unlike the situation in solution, this energy is not easily lost and so will be available to help the fragment traverse the transition state for C-C cleavage, shown in Figure 3. After dissociation, the role of Hg is negligible and so we only consider the isolated Ph-Et\* fragment. In the final step of the reaction the C-C bond breaking will take place at the weakest bond in the system, which in

this case is the  $\alpha,\beta$ -C-C bond in the ethyl substituent, because the resulting benzylic radical is strongly stabilized by resonance. Any other arene C-C bonds should be somewhat stronger, and the C-H bonds should be substantially stronger.

For Ph-Et\*, very similar transition states for the C-C cleavage step were located at both the MP2 and B3LYP levels. One imaginary frequency was found of  $828\text{ cm}^{-1}$  in the computed Hessian at the B3LYP level. The computed barrier for C-C activation of Ph-Et\* after zero-point corrections (at the B3LYP level) is 17.8 kcal/mol at the PCI-80 level. This barrier is substantial and can only be overcome at a reasonable rate within the lifetime of the triplet state because of the large excess vibrational energy of ca. 30 kcal/mol carried by Ph-Et\*. The exothermicity of the C-C bond breaking step in Ph-Et\* is 9.0 kcal/mol at the PCI-80 level, including a substantial zero-point vibrational effect of 7.2 kcal/mol.

**Electronic Structure of the Triplet Arene.** To break the  $\alpha,\beta$ -C-C bond of  $[\text{Ph-Et}]^*$ , a radical electron has to be transferred from the ring to the departing methyl group. This process is favored if (i) the ring carbon bearing the R substituent has substantial radical character, and, even more importantly, (ii) there is

Table 3

Substrate	Major Products	Rate of Product Formation (mg/h)	$\tau$
	isomers of MW 132 3.0% addition of H <sub>2</sub> O 5.9%  1.3%  60%  2.0% Partially saturated dimer 18.0% Fully saturated dimer 1.3%	3.3	3.30
	 4.2%  5.1% Dimers MW 236 76.8%	0.65	0.0
	 74.3%	0.30	0.0
	 3.5%  3.8%  61.4%  21.9%	2.29	2.98
	 13.7%  6.8%  15.5%  40.7%	2.8	1.32
	 trace  19.9%  37.4%	1.20	0.53
2-ethylpyridine } 4-ethylpyridine }	no noticeable reaction	<0.1	0.0

**Table 4. Energies (kcal/mol) at both the PCI-80 and B3LYP Levels for Intermediates Appearing in the Reaction between Ph-Et and Hg\***<sup>a</sup>

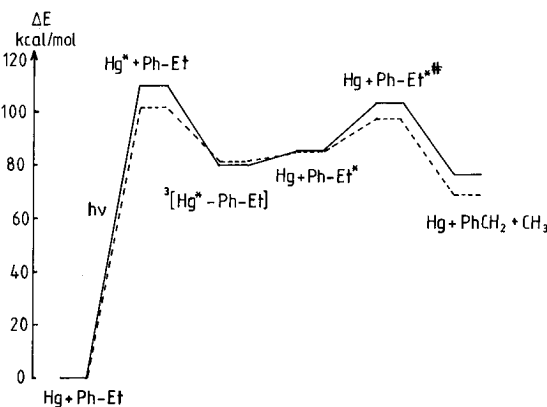
system	PCI-80	B3LYP	system	PCI-80	B3LYP
Hg + Ph-Et	0.0	0.0	Hg + Ph-Et	87.3	86.7
Hg* + Ph-Et	109.5	101.6	Hg + [Ph-Et*] <sup>‡</sup>	105.1	99.1
3[Hg* - Ph-Et]	79.6	81.1	Hg + Ph=CH <sub>2</sub> + CH <sub>3</sub>	78.3	69.7

<sup>a</sup> The energies are given relative to ground-state Hg and Ph-Et. Zero-point vibrational effects were obtained at the MP2 level.

overlap between the ring  $\pi^*$  orbitals and the antibonding C-C orbital of the ethyl group. This latter point implies that the C-C bond to be cleaved has to be perpendicular to the ring, as has recently been suggested in an experimental study by Otsuji and co-

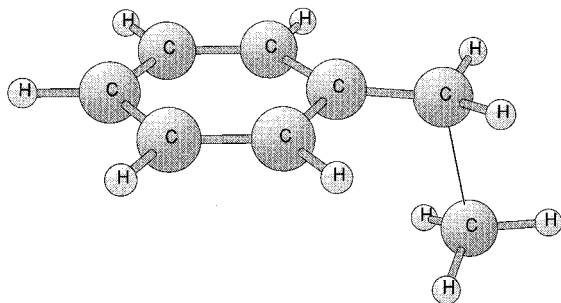
(6) Ichinose, N.; Mizuno, K.; Otsuji, Y.; Tachikawa, H. *Tetrahedron Lett.* **1994**, 35, 587 and references cited within.

(7) Comparing the barrier in indane with those in PhEt and C<sub>6</sub>H<sub>4</sub>-Et<sub>2</sub> suggests that 2.6 kcal/mol of the larger barrier height for indane results from the localization of the radical electrons on the ring, compared to 5.1 kcal/mol from the overlap effect, which is therefore the dominant contribution. The reaction exothermicities for C-C activation of the triplet (indane, 15.1 kcal/mol; PhEt, 16.3 kcal/mol) were not significantly different.



**Figure 2.** Energetics of the Hg\*/PhEt system from quantum chemical calculations at the PCI-80 level (full line) and B3LYP level (dotted). # indicates transition state for cleavage.

workers.<sup>6</sup> For Ph-Et both these requirements are fulfilled. The diradical character of the ring in [Ph-Et]\* leads to high radical character at the ethyl substituent and at the carbon opposite this position (see further below). The ethyl group can also easily rotate



**Figure 3.** Transition state for C–C bond cleavage in triplet state PhEt from quantum chemical calculations.

to become perpendicular to the plane of the aryl ring, which leads to a very favorable overlap between the radical orbital and the antibonding C–C orbital.

In Table 4 and Figure 2, the B3LYP and PCI-80 results are given in parallel. For the larger systems to be discussed below, the more economic B3LYP method has been used exclusively. As seen in Figure 2, the B3LYP results give a similar picture to the PCI-80 results for the entire reaction. The largest deviation of 5.4 kcal/mol occurs for the C–C activation step. Even if this difference is not negligible, the most important result in the following will be trends rather than absolute values and we conclude that the B3LYP method is quite sufficient for this purpose.

**Role of the Reactant Triplet Arene.** The formation of the  $\text{Hg}^*$ -arene exciplex leads to energy transfer from  $\text{Hg}^*$  to the arene. For this to take place, the reactant must have a triplet excited state at lower energy than that of  $\text{Hg}^*$  (theoretical, 109.5 kcal/mol; experimental, 112.7 kcal/mol). This requirement excludes C–C activation in alkanes, which have no such excited state. To illustrate this point, 1,2-dimethylbutane has a central C–C bond which is slightly weaker (B3LYP, 69.9 kcal/mol; experimental, 77.7 kcal/mol) than the weakest C–C bond of Ph–Et (experimental, 78.2 kcal/mol). However, no C–C cleavage occurs because the lowest excitation energy for 1,2-dimethylbutane (188.7 kcal/mol at the B3LYP level with a basis set including diffuse s- and p- functions) is far higher than the  $\text{Hg}^*$  energy (experimental, 112.7 kcal/mol).

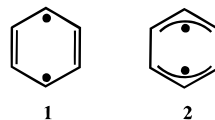
**Absence of C–C Cleavage in Dialkylarenes.** No C–C activation was observed in dialkylarenes. Three different explanations are possible: (i) The transition state energy may be much higher for dialkylarenes. (ii) The dialkylarenes have additional vibrational modes that prevent sufficient energy from concentrating in the scissile C–C bond within the lifetime of the triplet state. (iii) The excited-state lifetimes in dialkylarenes are much shorter.

To test explanation (i), we carried out a barrier height calculation for  $\text{C}_6\text{H}_4\text{Et}_2$ . The results of the B3LYP calculations for  $p\text{-C}_6\text{H}_4\text{Et}_2$ , given in Table 5, show that at the same level of approximation (B3LYP energies with Hartree–Fock zero-point vibrational effects), the barrier for the para-form is very similar to the barrier for Ph–Et, 15.0 kcal/mol compared to 15.2 kcal/mol. There are two alternative types of diradical states for the triplet arene: **1** and **2**. Since the radical tends to be localized at the substituted carbon, it is clear that Ph–Et and  $p\text{-C}_6\text{H}_4\text{Et}_2$  have essentially the same electronic structure, that of **1**. This is also the optimal position for the radical electron to activate the ethyl

**Table 5. B3LYP Energies (kcal/mol) for the C–C Activation Reaction of Ph–Et, of the *para* and *ortho* Forms of the Ph–Et<sub>2</sub>, and of Indane<sup>a</sup>**

reacn	B3LYP
Ph–Et $\rightarrow$ [Ph–Et*] <sup>‡</sup>	15.2
Ph–Et $\rightarrow$ Ph=CH <sub>2</sub> + CH <sub>3</sub>	–16.3
Ph–Et <sub>2</sub> ( <i>para</i> ) $\rightarrow$ [Ph–Et <sub>2</sub> *] <sup>‡</sup>	15.0
Ph–Et <sub>2</sub> ( <i>ortho</i> ) $\rightarrow$ [Ph–Et <sub>2</sub> *] <sup>‡</sup>	17.6
indane* $\rightarrow$ indane* <sup>‡</sup>	22.9
indane* $\rightarrow$ (C <sub>6</sub> H <sub>4</sub> )(C <sub>2</sub> H <sub>4</sub> )(CH <sub>2</sub> )	–15.1

<sup>a</sup> The energies are given relative to triplet ground states of the reactants. Zero-point vibrational effects were obtained at the Hartree-Fock level. ‡ = transition state.



**Figure 4.** Electronic structures of the two alternative triplet states for arenes.

C–C bond (see above). Ph–Et and  $p\text{-C}_6\text{H}_4\text{Et}_2$  will therefore have similar low barriers for C–C activation.

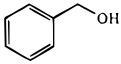
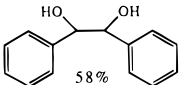
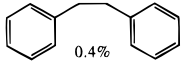
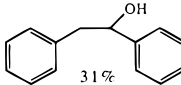
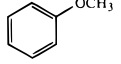
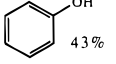
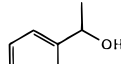
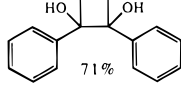
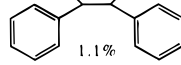
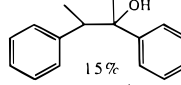
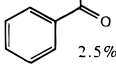
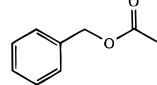
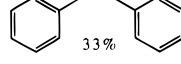
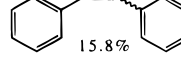
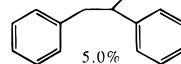
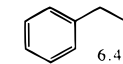
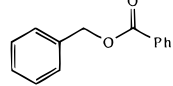
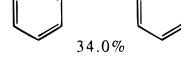
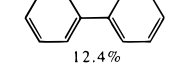
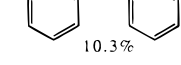
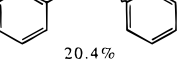
These results force us to eliminate explanation (i) above. On the dynamical explanation (ii), the excess vibrational energy of the newly formed  $\text{PhR}^*$  triplet is shared over less vibrational modes in PhEt than in  $\text{C}_6\text{H}_4\text{Et}_2$ . In confirmation of this idea, the amount of C–C cleavage falls off rapidly as the chain length of PhR increases (Table 2), implying a relation between C–C cleavage and the number of modes among which the vibrational energy is shared. As the number of modes increases, it becomes less likely that sufficient energy will concentrate in the scissile C–C bond. There is no evidence that the triplet lifetime is strongly affected by the chain length of R. Explanation (iii) is less likely but cannot be excluded.

Indane does not give any C–C activation with  $\text{Hg}^*$ . One possible reason is that *o*-disubstituted arenes might intrinsically have a substantially higher barrier for C–C cleavage. In *o*- and *m*- $\text{C}_6\text{H}_4\text{Et}_2$ , neither of the structures **1** or **2** of Figure 4 has the radical electrons entirely at *o*- and *m*-carbons, so the electronic structure should indeed be less favorable to C–C cleavage. The geometry optimization shows that the *o*- $\text{C}_6\text{H}_4\text{Et}_2$  triplet structure of type **2** is preferred. As expected, the barrier for C–C cleavage is somewhat higher, 17.6 kcal/mol, compared to 15.0 kcal/mol for  $p\text{-C}_6\text{H}_4\text{Et}_2$ .

Another possible factor is that the indane conformation prevents the C–C bond to be broken from becoming perpendicular to the arene ring, leading to poor overlap between the aryl  $\pi^*$ -orbitals and the antibonding C–C orbital. The singlet ground state is planar and therefore has zero overlap between these orbitals, although the more relevant triplet state of indane is slightly nonplanar, with the 2-carbon about 0.5 Å out of the molecular plane, but the overlap is still very poor compared to  $\text{C}_6\text{H}_4\text{Et}_2$  where the ethyl groups are free to rotate. The B3LYP barrier for indane is 5.3 kcal/mol higher than for the *o*- $\text{C}_6\text{H}_4\text{Et}_2$ , thus confirming our main conclusions.

**Experimental Results in C–Heteroatom Cleavage. C–Si Bond Cleavage.** C–Si bond strengths should be somewhat weaker than those of the corresponding C–C bonds, and these substrates were expected to give significant C–Si cleavage. Benzyltrimethylsilane did give substantial C–Si cleavage ( $r_{\text{CSi}} = 1.32$ ), compared to ethylbenzene ( $r_{\text{CC}} = 0.15$ ), but not

Table 6

Substrate	Major Products	Rate of Product Formation (mg/h)	$r$
	 58%  0.4%  31%	10	0.54
	 43% dimers 18% phenol dimers 40%	1.4	4.7
	 71%  1.1%  15%  2.5%	12	0.23
	 33%  15.8%  5.0%  6.4%	0.7	very high
	 34.0%  12.4%  10.3%  20.4%	0.21	very high

relative to the better benchmark,  $\text{PhCH}_2\text{CMe}_3$  ( $r_{\text{CC}} = 41$ ) (Table 3). Aromatic rings containing heteroatoms were also examined. While 2-ethylpyridine and 4-ethylpyridine gave no products, 2-ethylthiophene gave significant amounts of C–C bond cleavage (20%). Dehydrodimers were also formed (37%).

**C–O Bond Cleavage.** C–O bonds proved to be readily cleaved. Benzyl alcohol gave 58% of the normal C–H bond cleavage dehydrodimer, 1,2-diphenylethane-1,2-diol (Table 6). Substantial amounts of C–O bond cleavage products were also formed, however: 1,2-diphenylethanol (31%) and biphenyl (0.4%).  $r_{\text{CO}}$  for this substrate was 0.54, where  $r_{\text{CO}}$  is the ratio of  $R_{\text{CO}}$  groups, formed by C–O bond breaking, to  $R_{\text{CH}}$  groups, formed by C–H bond breaking. This result shows there is a slight preference for C–O cleavage in  $\text{PhCH}_2\text{OH}$  over the C–C cleavage of ethylbenzene ( $r_{\text{CC}} = 0.15$ ) (Table 6). In a competition experiment using *sec*-phenethyl alcohol, in which either the C–C or the C–O bond can cleave, only C–O bond cleavage products are seen. This demonstrates a large preference for C–O bond cleavage over C–C bond cleavage, the expected outcome due to the lower bond strength of C–O.

In the case of anisole, in which the positions of the  $-\text{CH}_2-$  and  $-\text{O}-$  groups are switched from that in  $\text{PhCH}_2\text{OH}$ , large amounts of the cleavage product, phenol, were formed (43%). Some dimers of anisole and of phenol were also seen (18% and 40%, respectively).  $r_{\text{CO}}$  for this reaction was 4.7, slightly higher than with the benzyl-substituted substrates of above.

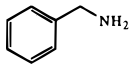
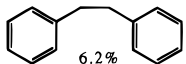
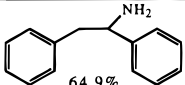
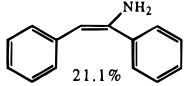
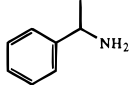
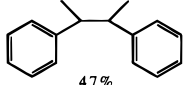
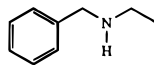
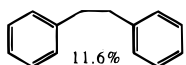

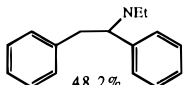
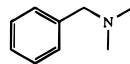
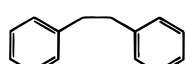
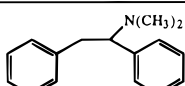
With acetate as leaving group, C–O bond cleavage seems to occur more readily. Benzyl acetate gave

biphenyl as the major product, with small amounts of stilbene also detected. In the case of benzyl benzoate, the products contain not only benzyl groups but also phenyl groups arising from decarboxylation of  $\text{PhCO}_2$  radicals: biphenyl (34.0%), diphenylmethane (10.3%), biphenyl (12.4%), and stilbene (20.4%). In all cases,  $r_{\text{CO}}$  was very high, no C–H bond cleavage products being detected.

**C–N Bond Cleavage.** C–N bond cleavage was only slightly less favorable than C–O cleavage. Benzylamine generated only the cleavage products, biphenyl (6.2%), 1,2-diphenylethylamine (64.9%), and 1,2-diphenylamine (21.1%); no C–H bond cleavage products were detected (Table 7). The  $r_{\text{CN}}$  value for this substrate is therefore very high. The case of methylbenzylamine allows us to compare C–C versus C–N bond cleavage. As in the C–O case, no C–C bond cleavage was detected. Cleavage of the C–N bond was complete; the major product detected was 2,3-diphenylbutane (47%). Some isomers of methylbenzylamine were also seen (8.9%).

Substitution on the nitrogen has little effect on the outcome. A secondary amine was examined first. *N*-ethylbenzyl amine led to some C–N cleavage products ( $r_{\text{CN}} = 0.27$ ). The tertiary amine *N,N*-dimethylbenzylamine gave significant amounts of C–N bond cleavage products: biphenyl (56.8%) and 1,2-diphenyl-1-(dimethylamino)ethane (13.9%). No C–H cleavage products were identified, so  $r_{\text{CN}}$  was not calculated.

Table 7

Substrate	Major Products	Rate of Product Formation (mg/h)	$\tau$
	 6.2%  64.9%  21.1%	5.75	very high
	 47% MW 120 isomers 8.9%	8.14	very high
	 11.6%  1.6%  48.2%	3.03	0.27
	 56.8%  13.9% MW 224 22.7%	15.0	very high

## Conclusion

We show that C–X cleavage reactions take place in  $\text{ArCH}_2\text{--X}$  ( $\text{X} = \text{alkyl, OR, NR}_2$ ) and related species on Hg photosensitization in the order  $\text{C--O} > \text{C--N} > \text{C--C}$ . Theoretical studies allow us to trace the reaction mechanism in some detail. The key step is the formation of an organometallic exciplex, having an  $\text{Hg}(\eta^2\text{-ArCH}_2\text{--X})$  structure. This dissociates to give a vibrationally excited triplet arene which then undergoes C–X bond cleavage. Dialkylarenes fail to give C–C cleavage, for which we propose a dynamical explanation.

## Experimental Section

NMR spectra were determined on a QE-Plus 300-MHz or Bruker 250-MHz instrument, and GC–MS analyses were carried out on an HP 5890 gas chromatograph (29 m, 0.25 mm id capillary column coated with a 0.25  $\mu\text{m}$  film of SE 30) connected with a HP 5972A MS detector. Substrates were distilled prior to use or, if new, used as received from Aldrich Co., PCR, Inc., or Kodak Corp. **Caution:** Mercury vapor is toxic, and appropriate precautions must be taken. No organomercury species were detected in the products, but they are saturated with Hg, which can be removed with Zn dust.

**Details for Individual Compounds. General Method.** Substrates (always in excess, starting weight or volume shown for each case) were placed in the quartz tube in a 1:5 ratio with distilled  $\text{H}_2\text{O}$ . A small drop of Hg was added, and the system was degassed via argon or  $\text{N}_2$  bubbling. The bottom of the quartz tube was then placed in the photoreactor and submerged in an oil bath.  $\text{N}_2$  or argon was passed into the system through a needle. The system was heated to reflux. The lamps were then turned on (four 8-W low-pressure lamps, 254 nm).

Products were collected by condensation inside the quartz reaction vessel. A condenser was used in each case. The organic products were extracted from the water with methylene chloride. The organic layer was then dried over  $\text{MgSO}_4$  and condensed. Monomer remaining in the mixture was then removed by either short path or Kugelrohr distillation, under reduced pressure when necessary. The extent of reaction was judged by the weight of the crude fraction isolated, taking into

account any traces of monomer remaining. All mixtures were analyzed by GC/MS.

Products were identified by comparison with authentic samples or literature data and confirmed by  $^1\text{H}$  NMR,  $^{13}\text{C}$  NMR, and/or GC/MS. GC/MS was used most frequently since product mixtures were complex and difficult to separate. NMR data are in chloroform unless stated. The data are reported as follows. Substrate: volume, photolysis time (temperature, atmosphere), major products and percentage in involatile fraction (GC), NMR, and MS. MS data are reported as the three major signals [ $m/z$  (relative intensity)].

**Mesitylene:** 0.5 mL in 2.5 mL  $\text{H}_2\text{O}$ , 22 h (100  $^\circ\text{C}$ ,  $\text{N}_2$ ), 73% mesitylene dimer, MS 238 ( $\text{MH}^+$ , 8), 119 (100), 84 (21).

**4-Phenyl-1-butene:** 0.5 mL in 2.5 mL  $\text{H}_2\text{O}$ , 13.5 h (100  $^\circ\text{C}$ ,  $\text{N}_2$ ), 3.0% isomer of phenylbutene, MS 132 ( $\text{MH}^+$ , 37), 104 (67), 91 (100), 5.9% phenylbutene alcohol, MS 150 ( $\text{MH}^+$ , 14), 117 (100), 91 (66), 1.3% phenylbutane, MS 134 ( $\text{MH}^+$ , 40), 91 (100), 2038 (17), 1.7% bibenzyl, MS 182 ( $\text{MH}^+$ , 42), 91 (100), 65 (12), 60% 1,2-diphenylpentene and isomers, MS (i) 222 ( $\text{MH}^+$ , 0.4), 117 (17), 91 (100), (ii) 222 ( $\text{MH}^+$ , 0.7), 105 (35), 91 (100), 2.0% 1,2-phenylpentane, MS 224 ( $\text{MH}^+$ , 33), 133 (12), 91 (100), 18.0% partially saturated dimers, MS (iii) 264 ( $\text{MH}^+$ , 3), 117 (29), 91 (100), (iv) 264 ( $\text{MH}^+$ , 3), 117 (29), 91 (100), 1.3% 4,5-diphenyloctane, MS 266 (23), 105 (17), 91 (8304).

**Cyclopropylbenzene:** 0.5 mL in 2.5 mL  $\text{H}_2\text{O}$ , 17 h (100  $^\circ\text{C}$ ,  $\text{N}_2$ ), 4.2% 1-phenyl-1-cyclopropanol, MS 134 ( $\text{MH}^+$ , 59), 133 (100), 117 (36), 5.1% 1-phenyl-1-propanol, MS 136 ( $\text{MH}^+$ , 22), 104 (100), 79 (69), 76.8% MW 236 dimers, MS (i) 236 ( $\text{MH}^+$ , 0.7), 167 (100), 131 (63), (ii) 236 ( $\text{MH}^+$ , 0.9), 118 (100), 91 (15), (iii) 236 ( $\text{MH}^+$ , 4), 118 (100), 91 (14), (iv) 236 ( $\text{MH}^+$ , 5), 118 (100), 91 (24), (v) 236 ( $\text{MH}^+$ , 26), 145 (100), 117 (46), (vi) 236 ( $\text{MH}^+$ , 11), 145 (100), 91 (29).

**Cyclohexylbenzene:** 0.5 mL in 2.5 mL  $\text{H}_2\text{O}$ , 18.5 h (100  $^\circ\text{C}$ ,  $\text{N}_2$ ), 74.3% 1-phenyl-1-cyclohexanol and isomer, MS (i) 176 ( $\text{MH}^+$ , 50), 149 (56), 133 (100), (ii) 176 ( $\text{MH}^+$ , 41), 149 (100), 104 (89).

**Methyl phenylacetate:** 0.5 mL in 2.5 mL  $\text{H}_2\text{O}$ , 16.5 h (100  $^\circ\text{C}$ ,  $\text{N}_2$ ), 3.5% phenyl acetic acid, MS 136 ( $\text{MH}^+$ , 39), 91 (100), 51 (15), 3.8% bibenzyl, MS 182 ( $\text{MH}^+$ , 31), 91 (100), 51 (12), 61.4% methyl 2,3-diphenylpropanoate and isomers, MS (i) 240 ( $\text{MH}^+$ , 25), 181 (24), 91 (100), (ii) 240 ( $\text{MH}^+$ , 4), 151 (23), 91 (100), (iii) 240 ( $\text{MH}^+$ , 43), 180 (75), 84 (100), (iv) 240 ( $\text{MH}^+$ , 3), 198 (100), 79 (77), (v) 240 ( $\text{MH}^+$ , 12), 198 (20), 84 (100), 21.9% dimethyl 2,3-diphenylsuccinate and isomers, MS (i) 298 ( $\text{MH}^+$ ,

2), 149 (71), 121 (100), (vii) 298 (MH<sup>+</sup>, 1), 149 (67), 121 (100), (viii) 298 (MH<sup>+</sup>, 8), 239 (54), 84 (100).

**Benzyltrimethylsilane:** 0.5 mL in 2.5 mL H<sub>2</sub>O, 14 h (100 °C, N<sub>2</sub>), 13.7% *bibenzyl*, MS 182 (MH<sup>+</sup>, 34), 91 (100), 84 (64), 40.7% *1-phenyl-1-(trimethylsilyl)methanol and isomers*, MS (i) 180 (MH<sup>+</sup>), 84 ( ), 51 ( ), (ii) 180 (MH<sup>+</sup>, 15), 135 (100), 73 (83), (iii) 180 (MH<sup>+</sup>, 45), 105 (28), 84 (100), 6.8% *1,2-diphenyl-1-(trimethyl)silylethane*, MS 254 (MH<sup>+</sup>, 9), 84 (100), 73 (48), 15.5% *1,2-diphenyl-1,2-bis(trimethylsilyl)ethane and isomers*, MS (iv) 326 (MH<sup>+</sup>, 10), 84 (47), 73 (100), (v) 326 (MH<sup>+</sup>, 8), 84 (100), 73 (85), (vi) 326 (MH<sup>+</sup>, 4), 223 (28), 84 (100).

**2-Ethylthiophene:** 0.5 mL in 2.5 mL H<sub>2</sub>O, 19 h (100 °C, N<sub>2</sub>), trace *1,2-bis(thiophene)ethane*, 19.9% *1,2-bis(thiophene)propane*, MS 208 (MH<sup>+</sup>, 6), 179 (94), 84 (100), 37.4% *2,3-bis(thiophene)butane and isomer*, MS (i) 222 (MH<sup>+</sup>, 28), 207 (91), 84 (100), (ii) 222 (MH<sup>+</sup>, 48), 207 (71), 84 (100).

**2-Ethylpyridine:** 0.5 mL in 2.5 mL H<sub>2</sub>O, 16 h (100 °C, N<sub>2</sub>), no products detected.

**4-Ethylpyridine:** 0.5 mL in 2.5 mL H<sub>2</sub>O, 16 h (100 °C, N<sub>2</sub>), no products detected.

**Benzyl alcohol:** 0.5 mL in 2.5 mL H<sub>2</sub>O, 12.5 h (100 °C, N<sub>2</sub>), 58.4% *hydrobenzoin and isomers*, 4.27–4.30 (m, 1H), 4.78, 4.82 (m, 1H), 7.15–7.24 (m, 10H), MS (i) 214 (MH<sup>+</sup>, 0.2), 108 (100), 79 (81), (ii) 214 (MH<sup>+</sup>, 0.2), 108 (100), 79 (82), (iii) 214 (MH<sup>+</sup>, 0.3), 92 (100), 79 (88), 30.9% *1,2-diphenylethanol and isomers*, 2.93–3.07 (m, 2H), 4.86, 4.88, 4.89, 4.90 (dd, 1H), 7.16–7.37 (10H), MS (iv) 198 (MH<sup>+</sup>, 1), 107 (84), 92 (100), (v) 198 (MH<sup>+</sup>, 0.4), 91 (100), 79 (22), (vi) 198 (MH<sup>+</sup>, 11), 167 (17), 91 (100), 0.37% *bibenzyl*, 2.89 (s, 4H), 7.16 (s, 10H), MS 182 (MH<sup>+</sup>, 27), 91 (100), 84 (42).

**Anisole:** 0.5 mL in 2.5 mL H<sub>2</sub>O, 12.5 h, (100 °C, N<sub>2</sub>), 42.6% *phenol*, MS 94 (MH<sup>+</sup>, 100), 66 (37), 65 (23), 39.9% *MW 186 isomers*, MS (i) 186 (MH<sup>+</sup>, 3), 184 (62), 84 (100), (ii) 186 (MH<sup>+</sup>, 3), 84 (100), 51 (21), (iii) 186 (MH<sup>+</sup>, 100), 84 (64), 51 (20), 17.5% *MW 214 isomers*, MS (iv) 214 (MH<sup>+</sup>, 18), 200 (38), 84 (100), (v) 214 (MH<sup>+</sup>, 7), 200 (21), 84 (100).

**sec-Phenethyl alcohol:** 0.5 mL in 2.5 mL H<sub>2</sub>O, (100 °C, N<sub>2</sub>), 70.6% *2,3-dihydroxy-2,3-diphenylbutane and isomers*, MS (i) 242 (MH<sup>+</sup>, <0.1), 121 (100), 77 (14), (ii) 242 (MH<sup>+</sup>, <0.01), 121 (100), 77 (17), (iii) 242 (MH<sup>+</sup>, 0.7), 121 (100), 84 (66), 15.4% *2,3-diphenyl-2-hydroxybutane and isomers*, MS (iv) 226 (MH<sup>+</sup>, 0.07), 121 (100), 77 (13), (v) 226 (MH<sup>+</sup>, 0.05), 121 (100), 77 (13), (vi) 226 (MH<sup>+</sup>, 0.5), 183 (100), 84 (80), 1.1% *2,3-diphenylbutane and isomers*, MS (vii) 210 (MH<sup>+</sup>, 2), 105 (100), 84 (61), (viii) 210 (MH<sup>+</sup>, 2), 105 (100), 84 (65), 2.5% *acetophenone*, MS 120 (MH<sup>+</sup>, 32), 105 (100), 77 (76).

**Benzyl acetate:** 0.5 mL in 2.5 mL H<sub>2</sub>O, 29 h (100 °C, N<sub>2</sub>), 6.4% *ethylbenzene*, MS 106 (MH<sup>+</sup>, 29), 91 (100), 77 (9), 33% *bibenzyl*, MS 182 (MH<sup>+</sup>, 24), 91 (100), 65 (12), 15.8% *1,2-diphenylethene*, MS 180 (MH<sup>+</sup>, 36), 149 (47), 107 (100), 5.0% *1-acetato-1,2-diphenylethane*, (i) 240 (MH<sup>+</sup>, 3), 207 (88), 107 (100), (ii) 240 (MH<sup>+</sup>, 4), 207 (100), 107 (94).

**Benzyl benzoate:** 0.5 mL in 2.5 mL H<sub>2</sub>O, 29 h (100 °C, H<sub>2</sub>O), 12.4% *biphenyl*, MS 154 (MH<sup>+</sup>, 33), 105 (100), 77 (62), *1,1-diphenylmethane*, MS 168 (MH<sup>+</sup>, 100), 122 (77), 105 (90), 34.0% *bibenzyl*, MS 182 (MH<sup>+</sup>, 38), 91 (100), 65 (9), 20.4% *1,2-diphenylethylene*, 180 (MH<sup>+</sup>, 50), 107 (83), 92 (100).

**Benzylamine:** 0.5 mL in 2.5 mL H<sub>2</sub>O, 14 h (100 °C), 6.2% *bibenzyl*, MS 182 (MH<sup>+</sup>, 45), 91 (100), 65 (13), 64.9% *1-amino-1,2-diphenylethane and isomer*, MS (i) 197 (MH<sup>+</sup>, 0.2), 106 (100), 79 (16), (ii) 197 (20), 106 (74), 91 (100), 21.1% *1-amino-1,2-diphenylethene*, 195 (MH<sup>+</sup>, 3), 106 (100), 79 (15).

**Methylbenzylamine:** 0.5 mL in 2.5 mL H<sub>2</sub>O, 15 h (100 °C, N<sub>2</sub>), 47% *2,3-diphenylbutane and isomers*, MS (i) 210 (MH<sup>+</sup>, 4), 119 (17), 105 (100), (ii) 210 (MH<sup>+</sup>, 3), 119 (28), 105 (100), (iii) 210 (MH<sup>+</sup>, 72), 105 (100), 77 (22), (iv) 210 (MH<sup>+</sup>, 70), 105 (100), 77 (20), 8.9% *MW 120 isomers*, MS (v) 120 (MH<sup>+</sup>, 17), 104 (100), 77 (25), (vi) 120 (MH<sup>+</sup>, 13), 77 (100), 51 (4), (vii) 120 (MH<sup>+</sup>, 100), 77 (11), 51 (4).

**N-Ethylbenzylamine:** 0.5 mL in 2.5 mL H<sub>2</sub>O, 29 h (100 °C, N<sub>2</sub>), 11.6% *bibenzyl*, MS 182 (MH<sup>+</sup>, 37), 91 (100), 65 (11), 1.6% *1,2-diphenylethene*, MS 180 (MH<sup>+</sup>, 35), 134 (70), 91 (100),

48.2% *1-N-ethyl-1,2-diphenylethane and isomer*, MS (i) 211 (MH<sup>+</sup>, 1), 195 (41), 91 (100), (ii) 211 (MH<sup>+</sup>, 49), 134 (15), 91 (100).

**N,N-Dimethylbenzylamine:** 0.5 mL in 2.5 mL H<sub>2</sub>O, 13 h (100 °C, N<sub>2</sub>), 56.8% *bibenzyl*, MS 182 (MH<sup>+</sup>, 40), 91 (100), 65 (11), 13.9% *1-N,N-dimethyl-1,2-diphenylethane and isomer*, MS (i) 225 (MH<sup>+</sup>, 19), 134 (100), 91 (20), (ii) 225 (MH<sup>+</sup>, 0.5), 134 (100), 91 (97), *MW 224 dimer*, MS 224 (MH<sup>+</sup>, 0.1), 134 (100), 91 (8).

**Computational Details.** Two types of calculations are reported, (i) *ab initio* and (ii) density functional theory (DFT) type based on hybrid functionals; both use standard quantum chemical methods with semiempirical corrections with one or only a few parameters. This type of parametrization has been shown to markedly improve the results compared to experiments. Basis sets of double  $\zeta$  plus polarization quality were used for the final energy evaluation in both the *ab initio* and the DFT calculations. The geometries were fully optimized at the DFT level using basis sets without polarization.

The *ab initio* calculations were performed using the recently developed PCI-80 method,<sup>8</sup> a parametrized scheme in turn based on calculations performed using the modified coupled pair functional (MCPF) method,<sup>9</sup> which is a standard quantum chemical, size-consistent, single reference state method. The zeroth order wave-functions were determined at the SCF level. All valence electrons were correlated including the 5d and 6s, 6p electrons on Hg. With double  $\zeta$  plus polarization (DZP) basis sets, it has been shown that about 80% of the correlation effects on bond strengths are obtained irrespective of the system studied. A good estimate of a bond strength is thus obtained by simply adding 20% of the correlation effects, and this is what is done in the PCI-80 scheme.<sup>8a</sup> The parameter 80 is thus empirical.<sup>10</sup> For several first-row systems it was shown in ref 8a that a Hartree–Fock limit correction is also strictly needed in the PCI-80 scheme. However, this correction has been shown to usually be small for heavy metal systems and a useful procedure is to consider these effects together with basis set superposition errors and core correlation effects as included in the parametrization. This procedure has been used in the present study. The PCI-80 calculations were performed using the STOCKHOLM set of programs.<sup>11</sup>

The DFT calculations were made using the empirically parametrized B3LYP method,<sup>12</sup> which uses the exchange functional of Becke,<sup>12</sup> the correlation functional of Lee, Yang, and Parr,<sup>13</sup> and the correlation functional of Vosko, Wilk, and Nusair.<sup>14</sup>

The introduction of gradient corrections and Hartree–Fock exchange and empirical parameters has made this type of hybrid DFT approach highly competitive in accuracy with the most accurate standard quantum chemical methods. Since the method uses Hartree–Fock exchange and has to compute some additional integrals, it is slightly slower than Hartree–Fock but normally slightly faster than MP2 and very much faster than more accurate standard correlation methods. This method was therefore used for most of the largest systems treated here, like the doubly substituted benzenes and for indane. The B3LYP calculations were carried out using the GAUSSIAN92/DFT package.<sup>15</sup>

(8) (a) Siegbahn, P. E. M.; Blomberg, M. R. A.; Svensson, M. *Chem. Phys. Lett.* **1994**, *223*, 35. (b) Siegbahn, P. E. M.; Svensson, M.; Boussard, J. *Chem. Phys.* **1995**, *102*, 5377.

(9) Chong, D. P.; Langhoff, S. R. *J. Chem. Phys.* **1986**, *84*, 5606.

(10) Pople, J. A.; Head-Gordon, M.; Fox, D. J.; Raghavachari, K.; Curtiss, L. A. *J. Chem. Phys.* **1989**, *90*, 5622.

(11) STOCKHOLM is a general purpose quantum chemical set of programs written by P. E. M. Siegbahn, M. R. A. Blomberg, L. G. M. Pettersson, B. O. Roos, and J. Almlöf.

(12) (a) Becke, A. D. *Phys. Chem. Rev.* **1988**, *A38*, 3098. (b) Becke, A. D. *J. Chem. Phys.* **1993**, *93*, 1372. (c) Becke, A. D. *J. Chem. Phys.* **1993**, *98*, 5648.

(13) Lee, C.; Yang, W.; Parr, R. G. *Phys. Chem. Rev.* **1988**, *B37*, 785.

(14) Vosko, S. H.; Wilk, L.; Nusair, M. *Can. J. Phys.* **1980**, *58*, 1200.



In the *ab initio* calculations a relativistic effective core potential (RECP) developed by Wahlgren was used.<sup>16</sup> In this RECP the 4s, 4p, 5s, 5p, 5d, and 6s electrons are treated explicitly and a (14s, 11p, 8d, 3f) primitive basis is used. The 4s, 4p, 5s, and 5p orbitals are described by a single  $\zeta$  contraction, the 6s and 6p by a double  $\zeta$  contraction, and the 5d by a triple  $\zeta$  contraction. The f function was contracted to one giving a [4s, 4p, 3d, 1f] contracted basis for Hg. For carbon the primitive (9s, 5p) basis of Huzinaga<sup>17</sup> was used, contracted according to the generalized contraction scheme to [3s, 2p], and one d function was added with exponent 0.63. For hydrogen the primitive (5s) basis from ref 17 was used, augmented with one p function with exponent 0.8 and contracted to [3s, 1p].

In the B3LYP calculations an RECP according to Hay and Wadt was used for mercury.<sup>18</sup> In this RECP the valence 5d, 6s, and 6p orbitals are described by double  $\zeta$  contractions, and no f function is used. The carbon basis is the same as used for the *ab initio* calculations, while for hydrogen a primitive (4s, 1p) basis contracted to [2s, 1p] was used.

(15) Gaussian 92/DFT, Revision G.1: Frisch, M. J.; Trucks, G. W.; Head-Gordon, M.; Gill, P. M. W.; Wong, M. W.; Foresman, J. B.; Johnson, B. G.; Schlegel, H. B.; Robb, M. A.; Replogle, E. S.; Gomperts, R.; Andres, J. L.; Ragavachari, K.; Binkley, J. S.; Gonzales, C.; Martin, R. L.; Fox, D. J.; Defrees, D. J.; Baker, J.; Stewart, J. J. P.; Pople, J. A. Gaussian Inc.: Pittsburgh, PA, 1993.

(16) Wahlgren, U. To be published.

(17) Huzinaga, S. *Approximate Atomic Functions. II*; Department of Chemistry Report; University of Alberta: Edmonton, Alberta, Canada, 1971.

(18) Hay, P. J.; Wadt, W. R. *J. Chem. Phys.* **1985**, *82*, 299.

Hg is so heavy that a reasonable treatment of relativistic effects is absolutely necessary for good accuracy. On the basis of comparisons to relativistic all-electron no-pair calculations, the present RECP has been shown to perform very well.<sup>8b</sup> This is also verified for the spin-orbit average excitation energy which at the PCI-80 level becomes 116.3 kcal/mol compared to the experimental average value of 119.5 kcal/mol. The RECP should therefore account for all relativistic effects except for spin-orbit effects. In the previous study of Hg\* reactions<sup>4</sup> it was shown that a useful approximation of spin-orbit effects is to consider them as quenched for the molecular systems. The only exception to this rule occurs for the very weakly bound van der Waals complexes of alkanes and Hg\*. Spin-orbit effects will lead to a lowering of the energy by 6.8 kcal/mol, the difference between the calculated average value and the Hg\* <sup>3</sup>P<sub>1</sub> component. For the reaction products, spin-orbit effects will not lead to any lowering. It was shown earlier that zero-point vibrational effects can be quite important for these reactions.<sup>4</sup> In the present study these effects have been taken care of at the MP2 level for the smaller systems and at the Hartree-Fock level for the larger systems. The Hartree-Fock effects are scaled by a factor of 0.9, as usual.

**Acknowledgment.** We thank the Department of Energy for funding.

OM9507033